Chitosan-based formulations intended as masks surface protective spray for prevention of coronavirus dissemination

Victoria Belen Ayala-Peña[b], María Julia Martin[a, c], Florencia Favatela[a], Jessica Otarola[a], María Ventura[d], Claudia Gentili[c], María Florencia Salcedo[e], Andrea Mansilla[e], Sandra Pérez[f], Guillermina Dolcini[f], Vera Alvarez[g], and Verónica Lassalle*[a]

[a] PhD VL Lassalle, PhD MJ Martin, Dr. F Favatela, Dr, J Otarola
INQUISUR, Departamento de Química, Universidad Nacional del Sur (UNS)-CONICET.
Av. Leandro Niceforo Alem 1253, B8000 Bahía Blanca, Provincia de Buenos Aires. Argentina.
* e-mail: velassalle@gmail.com
[b] PhD. VB Ayala-Peña
INIBIBB, Departamento de Biología, Bioquímica y Farmacia, Universidad Nacional del Sur (UNS)-CONICET.
Camino La Carrindanga km 7, B8000, Bahía Blanca, Provincia de Buenos Aires, Argentina
[c] PhD MJ Martin, PhD C Gentili
INBIOSUR, Departamento de Biología, Bioquímica y Farmacia, Universidad Nacional del Sur (UNS)-CONICET
San Juan 671, B8000, Bahía Blanca, Provincia de Buenos Aires, Argentina.
[d] Dr M Ventura
IAE-Instituto Analítico Especializado
Córdoba 3935, B1653BJK, Villa Ballester - Pcia. de Buenos Aires. Argentina
[e] PhD. MF Salcedo, PhD A Mansilla
Instituto de Investigaciones Biológicas, UE-CONICET-UNMdP, Facultad de Ciencias Exactas y Naturales, Universidad Nacional de Mar del Plata.
Déan Funes 3240, B7600, Mar del Plata, Argentina.
[f] PhD S Perez, PhD G Dolcini
CIVETAN - CONICET, Facultad de Ciencias Veterinarias, UNCPBA,
Pje Arroyo Seco s/n campus universitario, B7000, Tandil, Argentina.
[g] PhD V Alvarez
INTEMA, Facultad de Ingeniería, Universidad Nacional de Mar del Plata (UNMdP)-CONICET.
Av. Cristóbal Colón 10850, B7600, Mar del Plata, Argentina.

Abstract: The extraordinary occurrence of COVID-19 by the fast expansion of SARS-CoV-2 infections has propelled particular interest in developing novel antiviral and virucidal agents to guarantee personal security. One of the main current challenges is to optimize the use of personal protection elements without the detriment of biosecurity. In recent years, chitosan (CH) has attracted attention for being an interesting multifunctional, biodegradable, non-antigenic, non-toxic, and biocompatible natural polymer with antimicrobial properties. In this work, formulations based on a CH matrix containing silver (Ag), and Copper (Cu) nanoparticles (CH@AgCuNPs) have been developed. The novelty of this proposal is that low viscosity formulations are reached, possessing antiviral and antibacterial bioactivity; hence they can be easily sprayed on various surfaces, including conventional face masks. The results presented in this contribution provide strong evidence on CH films as an ideal biosecure surface-covering for conventional masks.

Introduction

Since the COVID-19 pandemic started, one problem that has attracted global attention is the disruption or shortages of personal protective equipment. In particular, face masks are crucial elements for healthcare since they allow airborne pathogens filtration. In addition, these are useful tools to reduce the times that people touch their face / mouth / nose with unhygienic hands, significantly reducing the possibility of contracting respiratory infections [1,2]. The main route of transmission of SARS-CoV-2, like other respiratory viruses, is through viral particles loaded in droplets and excretions that are spread by coughing and breathing. Once these particles contact the mucous membranes or enter the respiratory tract, the virus can eventually infect host cells [3,4]. The easiness with which this type of virus can stay and travel through air currents implies a significant risk of transmission indoors and in crowded places places [5]. Recent reports describe that once expelled by the cough of an infected person, the estimated survival for SARS-CoV-2 in airborne droplets can be up to 3 h [6]. Given these facts, droplets and airborne transmission represent the main route of the spread of this and other similar viruses, and it can be interrupted through the use of personal protective equipment.

The use of disposable masks is crucial for the protection of healthcare workers to prevent occupational risks, however, non-medical workers adopted these protective elements during the COVID-19 pandemic and similar measures were used against other previous viral outbreaks [1,7–9]. Masks availability is and will continue being a challenge given the constant need for these limited elements. The high demand of face masks to slow down the transmission rate of COVID-19 has occasioned a global shortage of face masks for the most vulnerable groups, including the healthcare workers [10,11]. The number of masks required to respond to COVID-19 for health areas, according to data provided by the World Health Organization (WHO), is 89 million per month [12]. This demand has occasioned a record increase in the global production of polymeric face masks. Besides from 2020 (pandemic initiated) to date the residues related to personal care elements have multiplied exponentially, generating an additional environmental problem [13]. In this context, the need to offer more efficient, non-discernable and eco-friendly materials to revert this situation appears as a great

challenge from the scientific and the socio-productive environment.

The antimicrobial properties of chitosan are limited to its polymerization degree [14], however chitosan based formulations with antiviral activity have been extensively reported. Instead, only few research deals with antiviral capacities of chitosan against human viruses. Despite this, interesting advances have been made in this field [15].

Previous works with chitosan based formulations on and including silver nanoparticles have demonstrated their antibacterial [16,17], antifungal [18], and anti-influenza A virus [19] activity. However, the activity against coronavirus and herpes simplex type 1 of formulations based on chitosan with silver nanoparticles is described here for the first time, to the best of the author´s knowledge. *The in situ* formation of copper nanoparticles in the matrix of chitosan has already been described [20]. However, the antiviral activity of formulations based on chitosan- copper oxide nanoparticles was described for the first time in our previous work [21]. It is known that the combination of both metals (copper and silver) enhances the antibacterial activity of each one individually [22]. Morsi and coworkers proposed the preparation of chitosan-based compounds combined with carbon nanotubes containing copper and silver nanoparticles as antimicrobials for water treatment. They proposed that both nanoparticles greatly modify the chitosan charge density, increasing the possibilities of forming an impermeable layer around the microorganisms [23]. More et al obtained chitosan and polyvinyl alcohol fibers with silver and copper nanoparticles by electrospinning process [24]. After this survey, it is evident that there is not enough information regarding simple and scalable methods to obtain CH based formulations containing Ag and CuO nanoparticles to enhance their antiviral properties. Even more, the available literature reporting the use of these raw materials to achieve antiviral sprayable formulations is inexistent. Here, we describe the synthesis, characterization and analysis of viability of a novel spray, CH@AgCuNPs, based on chitosan containing two kinds of inorganic nanoparticles, obtained from a simplified methodology which allows its potential use at industrial level. This formulation was thought for easy application to any type of woven or non-woven fabric, and plastic surfaces.

To test the antiviral properties of CH@AgCuNPs, we have chosen two enveloped viruses *herpes simplex type 1* (HSV-1) and *bovine betacoronavirus* (BCoV). Viruses such as coronaviruses and herpesviruses are coated with a phospholipid bilayer envelope. Similar to SARS-CoV-2, BCoV is a member of the family *Coronaviridae*, which comprises positive-sense single-stranded RNA viruses. The selection of these viruses for this study is based on the requirement of laboratories with high biosecurity levels for the manipulation of SARS-CoV-2 to guarantee the personal biosafety. In this regard, other biotechnological developments in the current pandemic context have implemented similar strategies to evaluate the antiviral properties of biomaterials [25–27].

Since the main media where the antiviral activity was tested was the surface of face masks, we propose that implementing this kind of sprayable product would allow the face masks to be reused without the need of sterilization or their elimination after use. Therefore, the two major advantages attributable to CH@AgCuNPs spray formulations are the prevention of the spread of viruses, including SARS-CoV-2. Secondly, this technology will significantly contribute to the reduction of waste production.

Results and Discussion

Table 1. Different CH based formulations obtained by varying the Copper and Silver content

Formulation	Nomenclature	Metal concentration *	Cu concentration ** (mg/L)	Ag concentration ** (mg/L)
1	CH-Cu5	5%Cu	44.85	-
2	CH-Cu1	1%Cu	72.92	-
3	CH-Cu0.5	0.5%Cu	39.56	-
4	CH-Ag 5	5%Ag	-	365.91
5	CH-Cu-Ag 0.125	0.125%Cu 0.125%Ag	12.40	18.63
6	CH-Cu-Ag 0.25	0.25%Cu 0.25%Ag	25.65	32.79
7	CH-Cu -Ag 0.5	0.5%Cu 0.5% Ag	35.62	63.7

1. Characterization data

The initial stage in preparing the formulations according to the above described procedure involved a screening regarding the concentration of metallic salts employed. The main goal of this

Figure 1. Images of (a) chitosan-Cu1%, (b) chitosan-Ag-1% and (c) chitosan-Ag-Cu 0.25% formulations.

experimental procedure was to find the best conditions, in terms of metals/CH proportions to provide satisfactory antimicrobial/antiviral properties and suitable capability to adhere to different surfaces, including face masks. The combination of raw materials is depicted in Table 1. Those exhibit differences related to the metal content, which affects their physical aspect as well as their physicochemical properties. Figure 1 shows the physical appearance of the selected CH formulations, to better illustrate. As can be seen, materials with different appearances, and fundamentally viscosities were obtained.

From the analysis of **Figure 1** and data on metallic content achieved by AAE, it is clear that increasing the concentration of metallic salts the crosslinking level of CH grows up leading to formulations with hydrogel structure. The role of metallic salts to promote the biopolymeric crosslinking has been reported in open literature [28,29].

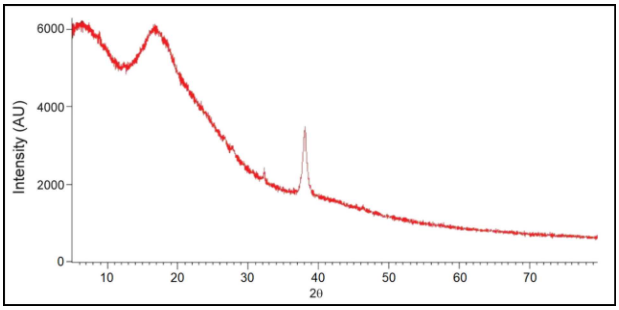

Figure 2. XRD diffractograms.

For instance, Kozicki et al has described the gelation of chitosan solution with silver nitrate. They found that above the critical concentration of chitosan (c*), continuous hydrogels of chitosan–silver can be formed. At lower concentrations, the formation of nano- and micro-hydrogels were obtained [30].

Based on the above discussed and considering the main goal of achieving a sprayable formulation, those of lower viscosity were selected, i.e 5-7. XRD diffractograms are depicted in **Figure 2** where the characteristic peak of chitosan was observed at 2θ = 19.9°, indicating high degree of chitosan and their crystal lattice constant α corresponding to 4.4. It is also noticeable the crystalline pattern of Ag and Cu moieties may be distinguished by the presence of Bragg reflection signal at 2θ 38.6 corresponding to (111) plane of Ag NPs (JCPDS card no: 65-2871). This evidence is in accordance with the findings of other authors who reported that the sharp peak can be associated to some bioorganic compounds/proteins present during NPs formation [18]. Besides the reflection planes that confirmed the presence of face-centered cubic form of metallic silver, other peaks may be distinguished at 2θ impurity crystalline phases were observed at 2θ 32 that may be assigned to the reflection of plane 110 of CuO. It is worth mentioning that the most important signal appearing in CuO XRD is associated to the plane (111) located at 2θ 38, overlapping in this case with the same plane (111) corresponding to the Ag NPs [20].

FTIR analysis was performed to estimate the changes originated in the functional groups of the polymeric moieties due to the metallic salts incorporation. Therefore, spectra of bare chitosan is shown in **Figure 3a** (as reference), and spectrum of formulations 5, 6 and 7 are included in **Figure 3b**.

In spectra included in both **Figure 3a** and **b** the typical CH bands are appreciated; i.e the broad absorption band between 3600 and 3000 cm-1, which is assigned to the stretching of -OH groups and -NH groups of the carbohydrate ring [31], the peaks at 1370 and1309 cm-1 to -CH bending vibrations, and the peak at 1069 cm^{-1} to the skeletal frequency of -C-O-C- [32]. Therefore, in **Figure 3b**, the bands described in **Figure 3a** are observed, with some variations. The signal at approximately 3400 cm^{-1} is broadened and slightly shifted due to the interaction with the metallic cations. Other specific peaks for chitosan are changed, either by reduction of intensity or shifting. The major change in the bands, at aprox. 1560 cm^{-1}, corresponding to the amino groups of chitosan, shifted to lower wavelength, suggesting that the mechanism involved between the metallic moieties and the biopolymer is mainly based on the coordination interaction of primary $–NH_2$ groups with the Cu and Ag cations. Besides, a sharp signal at 1450cm^{-1} appears associated to NO_3^- arising from $AgNO_3$ showing increasing intensity at higher metallic salt concentrations.

In general, the types of interactions between CH and metallic cations given within this work are compatible with the formation of cationic nanoparticles stabilized by the CH polymeric matrix [16,21].

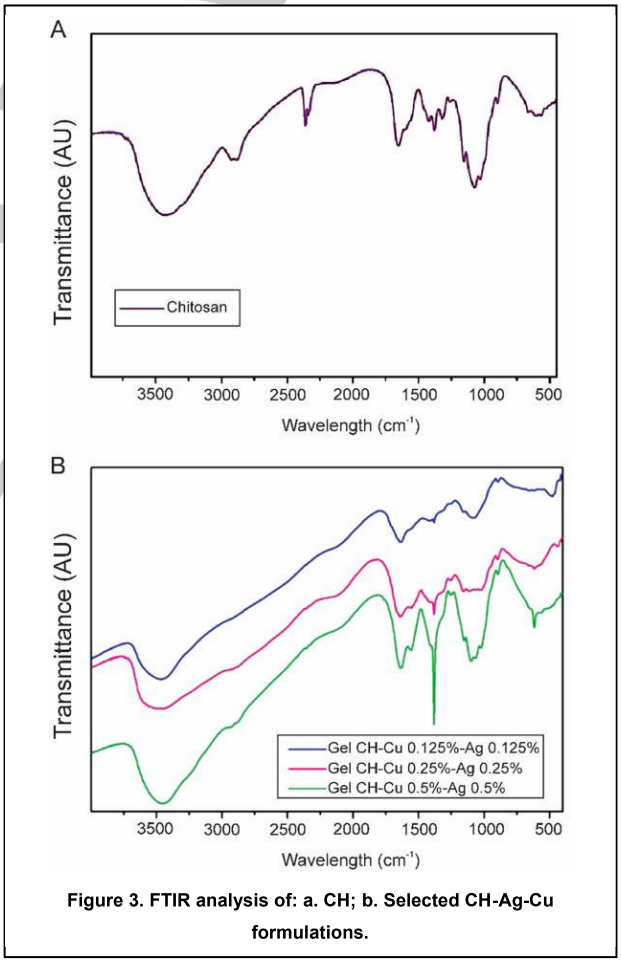

Figure 3. FTIR analysis of: a. CH; b. Selected CH-Ag-Cu formulations.

TEM micrographs of CH@AgCuNPs formulations are depicted in **Figure 4**. The TEM images suggest that the biopolymer acts as matrix where the inorganic nanoparticles remain dispersed. The role of the CH as nanoparticles stabilizer has been well documented in open literature [18]. The images included in **Figure 4** are compatible with well dispersed and homogeneous in shape nanoparticles, mainly ascribed to Ag NPs (**Figure 4a**), whereas the regions showing clusters or higher in size

aggregates of NPs are more likely ascribed to the formation of CuO NPs (**Figure 4b**). Data concerning hydrodynamic diameter measured by DLS, coincide with the results of TEM revealing that a bimodal distribution of sizes exists in most of evaluated samples which is compatible with the occurrence of two nanoparticles populations. Similar findings have been reached by other authors [17].

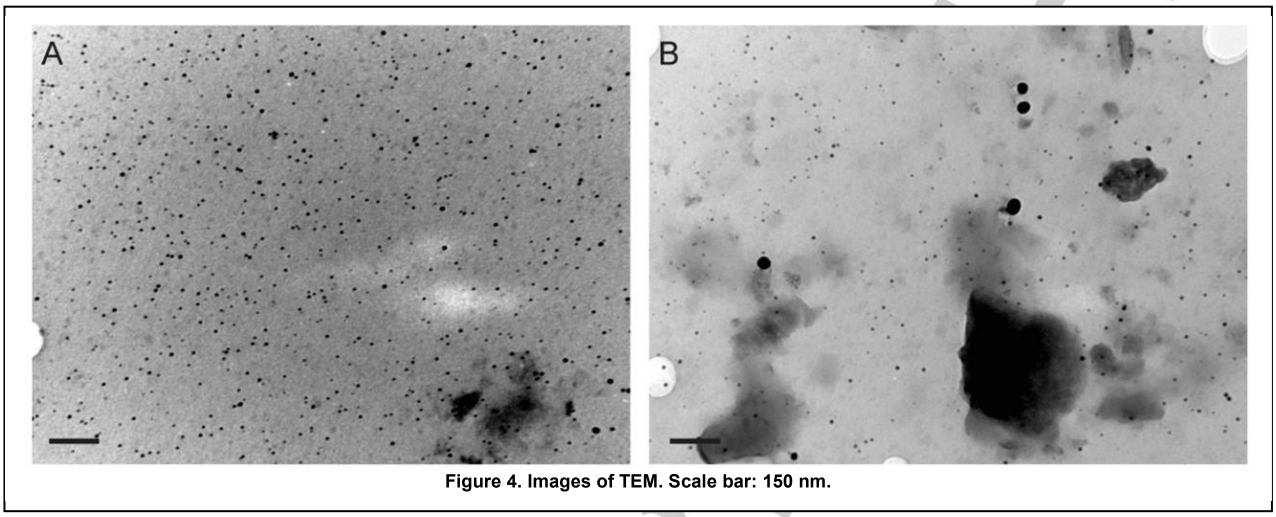

Figure 4. Images of TEM. Scale bar: 150 nm.

The values of Z potential measured at pH=5.70 ranged between 35 and 43 mV, indicating that exposed protonated amine groups of CH are present. This result further confirmed the structure of inorganic nanoparticles as incorporated and stabilized by means of the CH@AgCuNPs matrix.

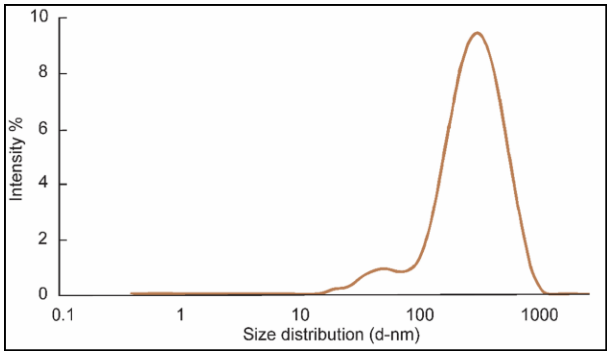

Figure 5. Size distribution of Gel CH-Cu 0,25%-Ag 0,25% (CH@AgCuNPs).

2 Biological studies

2.1 BCoV adsorption and desorption assays

The adsorption (binding) assay evaluates the ability of the CH@AgCuNPs to adsorb BCoV virions. On the other hand, the desorption test evaluates the CH@AgCuNPs ability to retain adsorbed viruses after desorbing agent treatment (2M NaCl) (Table 2). The surface of viruses may become charged due to their isoelectric point and pH of the environment. In this sense, the surfaces interactions with the adsorbents formulations may be primarily electrostatic or mostly hydrophobic [33]. CH manages a strong virus adsorption, thus, virus release needs a strong ionic solution such as 2M NaCl which retains virus virulence [34].

We have shown that in CH@AgCuNPs formulation, the desorbed viruses have null or very low (decrease in ~2 log) viral activity in concentrated or diluted solutions, respectively. The mechanism of action of Chitosan against microorganisms is not completely understood, but previous reports support the antiviral and antimicrobial activity. Several studies demonstrated that chitosan could block viral attachment to host cells [34–37].

Chitosan could interacts with the S protein of HCoV-NL63 and form a protein-polymer complex, which results in virus neutralization [36]. Previous studies demonstrated that nano/microspheres of N-(2- hydroxypropyl)-3-trimethyl chitosan (HTCC-NS/MS) strongly adsorb the particles of HCoV-NL63 virus, moderately adsorb mouse hepatitis virus (MHV) particles, but do not adsorb HCoV-OC43 [34]. Even though BCoV is a *betacoronavirus linage A* as HCoV-OC43, our CH formulation was able to inactivate a betacoronavirus linage A.

Table 2. BCoV titers after adsorption and desorption assay. Data represent theaverage of three independent experiments.

BCoV $TICID_{50}$/ml	Initial viral titer	Viral titer after adsorption	Viral titer after desorption
Concentrated	10^5	0	0
1:3 dilution	10^5	$10^{1.0\pm 1,7}$	$10^{3.07\pm 0,1}$

Others also reported that nanofibers of CH may be used to adsorb porcine parvovirus and sindbis virus [37>. In summary, here we determined the inactivation of HSV-1 induced by CH@AgCuNPs formulations. A study demonstrated that alpha-herpes virus mutants deleted in several glycoproteins had lost the ability to be adsorbed to different proteins and peptides [38], which suggests that HSV-1 could be absorbed by chitosan through its glycoproteins in a non-specific way, as it would happen for coronaviruses, inhibiting cell invasion.

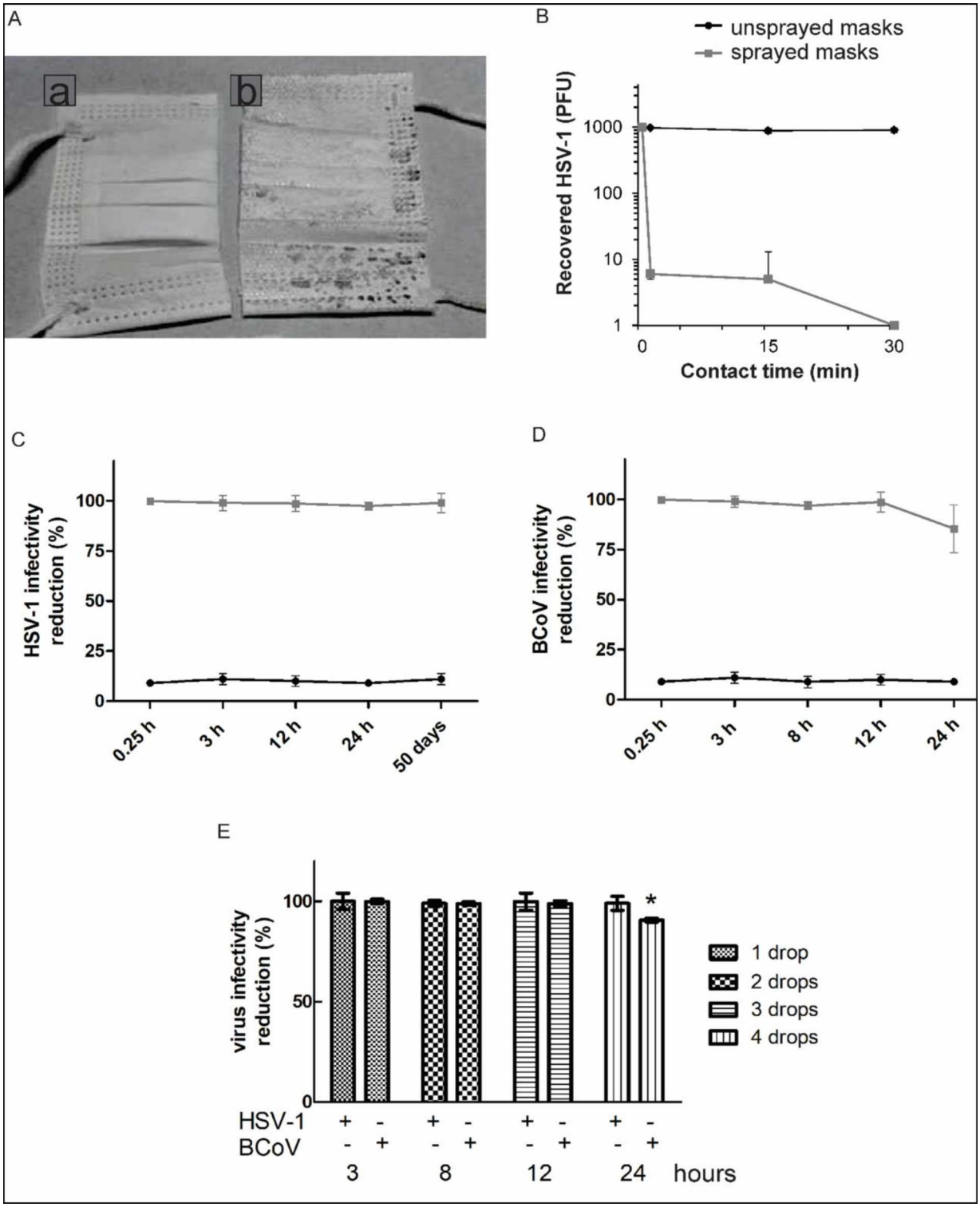

Figure 6. CH@AgCuNPs was used to spray-coat the mask surfaces. A) Photographs of unsprayed (a) and CH@AgCuNPs -sprayed (b) commercial masks, after one hour of depositing approximately 100 µl/cm^2. **B)** Persistence of infectious HSV-1 on sprayed or unsprayed surfaces. Approximately 10^3 PFU HSV-1 (one drop of 20 µl) was applied on 1 cm^2 of sprayed or unsprayed mask surfaces and incubated at ambient conditions (21°C; relative humidity, 30% to 40%) for various time points. **C)** and **D)** Persistence of virucidal activity of sprayed masks: evaluation of virus titers with respect to the spraying time. After each spraying time, approximately 10^3 PFU HSV-1 or BCoV was applied to 1 cm^2 of sprayed or unsprayed masks and incubated at ambient conditions for 5 minutes. E) Evaluation of virus titers in sprayed masks or unsprayed after repeated viral inoculum. 0 h was the initial spraying time. 3 h later one drop of HSV-1 or BCoV suspension were applied to 1 cm^2 and incubated at ambient conditions during 5 minute and the viral titer was evaluated. The procedure was repeated at 8, 12 and 24h (a total accumulation of 4 drops of virus suspension). For **B)**, **C)** and **E)** experiments we used CH@AgCuNPs formulation in a dilution 1:3; for **C)** experiment we employed a dilution 1:2. Error bars represent ± SEM, and data are from three independent experiments. *p< 0.05 vs control.

In our previous report Cu salts were selected as enhancers of antimicrobial activity [21]. Copper is known for its antimicrobial

property, and also proven to be capable of inactivating SARS-CoV-2 [6]. The antimicrobial activity of copper oxide is attributed to the generation of reactive oxygen species (ROS) [39]>. Here we incorporated Ag, a metal with power of antiviral activity; its antimicrobial mechanism is largely attributed to the release of Ag^+ ions upon contact with aqueous systems [40,41]. The antiviral activity has been related to the generation of ROS [42] and binding to viral proteins or to the direct lysis of membranes [43–46]. The metals presence could explain the improvement in this formulation against BCoV with respect to Ciejka formulations [34]. These studies suggest that the viral inactivation achieved by our formulations could be due to an unspecific interaction with viral glycoproteins preening the attachment to the host cell. On the other hand the metals could inactive the virus by ROS generation and/or lysing membranes. Overall, independently of the mechanism of action, formulations of rapid antiviral action were generated.

2.2 Evaluation of virus titers with respect to contact time in sprayed masks

In a series of experiments, we investigated the antiviral effect of CH@AgCuNPs formulation sprayed on masks surfaces. The surfaces were sprayed with CH@AgCuNPs formulations depositing approximately 100 µl/cm^2 (**Figure 6a**). When the CH@AgCuNPs formulation was dry, the surfaces were subjected to a UV cycle for 15 min and then viral infections were done. As shown in **Figure 6b**, an inoculum of 10^3 plaque forming units (PFU) of HSV-1 persisted on not-sprayed surfaces masks for at least 30 min at 21°C and relative humidity of 30% to 40%. Although the initial inoculum concentration was quite low, the virus retained infectivity for 30 minutes on not-sprayed surfaces. Rapid inactivation of HSV-1 occurs on CH@AgCuNPs -sprayed surfaces masks at room temperature (21°C). The rate of inactivation was > 2 log at 1 minute of contact (~99,5%). Approximately 10^3 PFU in simulated wet-droplet contamination (20 µl per cm^2) was inactivated in less than 30 min. However, unsprayed mask surfaces did not improve maximal viral inactivation.

2.3 Persistence of antiviral activity of sprayed surfaces masks

One of the current challenges for these types of materials lies in the development of universal virus repudiation systems that are reusable and with perdurable antiviral activity thus reducing the risk of infection and transmission. With the aim of studying the persistence of virucidal activity of sprayed surfaces masks, we evaluated the viral titers with respect to the spraying time (**Figure 6c** and **d**). As mentioned above, the antiviral tests were performed with HSV-1 and BCoV. We demonstrated that the CH@AgCuNPs sprayed masks surfaces keep an important virucidal activity up to 50 days for HSV-1 and moderated activity up to 24 h for BCoV. On the contrary, the surfaces of the unsprayed masks lack of virucidal activity. Currently, health personnel uses one individual mask per each people, during 24 hours. Thus, the replacement and disposal of masks can be exorbitant. Then, we proposed that in CH@AgCuNPs sprayed conditions, the use of the same chinstrap could be optimized for at least up to 24 hours.

2.4 Evaluation of virus titers after repeated viral inoculum in sprayed masks

Subsequent studies pointed to determine the antiviral activity of CH@AgCuNPs formulation after repeated viral inoculum in a determined time. Four drops of HSV-1, 1000 PFU/drop, were added four times during 5 days in sprayed surfaces masks (**Figure 6e**), and the % of reduction of viral titer was about 100% for coated masks regarding uncoated ones.

Consequently, we consider that the CH@AgCuNPs coatings are good candidates to be tested and authenticated, to fabricate a wide range of coated antiviral products such as masks, gowns, surgical drapes, textiles, high-touch surfaces, and other personal protective equipment. This would be particularly useful in the context of COVID-19 pandemic and for coating in using in critical areas like hospitals, healthcare centers, and crowded places and are promising to reduce the risk of coronavirus infection.

The sprayed masks surfaces decreased the titers of both virus ~100 %. These results were coincident with those obtained from masks sprayed without prior exposure to UV (data not shown). In this study, antiviral tests were performed against both DNA and RNA virus models which are HSV-1 and BCoV respectively. However, the specific mechanism of HSV-1 and BCoV inactivation of CH@AgCuNPs formulations needs to be studied in depth.

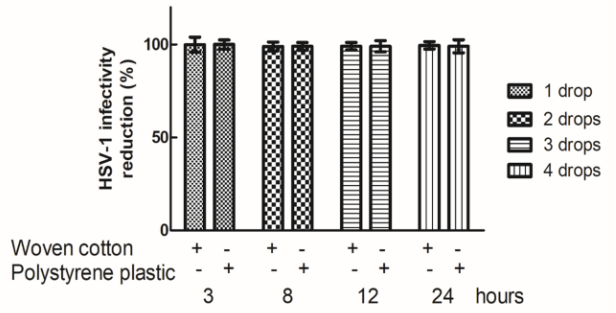

Figure 7. Evaluation of virus titers in masks sprayed or not after repeated viral inoculum. 0 h was the initial spraying time. 3 h later one drop of HSV-1 suspension was applied to 1 cm^2 and incubated at ambient conditions during 5 minute and the viral titer was evaluated; 8 h later a second drop was added on the same zone, and the viral titer was evaluated; 12 h later a third drop was added on the same zone and the viral titer was evaluated; 24 h later a fourth drop was added on the same zone and the viral titer was evaluated as described in the text. For these experiments a dilution 1:3 of CH@AgCuNPs formulation was used. Error bars represent ± SEM.

2.5. Evaluation of virus titers after repeated viral inoculum in others sprayed surfaces

Given that some face masks contain plastic elements and that, the use of homemade sanitary masks made of woven fabric has been massively used; we also performed antiviral studies on other surfaces such as woven cotton fabric and polystyrene plastic. Taking into account that this CH@AgCuNPs formulation ensures an antiviral activity within 24 hours for BCoV and longer times for HSV-1, we proceeded to study the behavior of this CH@AgCuNPs on woven cotton or polystyrene plastic surfaces during 24 hours with repeated HSV-1 inoculations (**Figure 7**). These results demonstrated that CH@AgCuNPs virucidal activity against HSV-1 is not affected when is sprayed on woven cotton fabric or polystyrene plastic. The antiviral action is similar to that observed when the CH@AgCuNPs had been sprayed on face masks (**Figure 7**). These studies show that these formulations can be applied to woven and non-woven fabrics as

well as to plastic surfaces with potential massive use on different surfaces.

We proceeded to study whether the type of storage container affected the CH@AgCuNPs virucidal activity. For this propose, we carried out a study of viral overload for 5 days in samples stored in plastic or glass containers. 0 h was the initial spraying time. 30 min later one drop of HSV-1 suspension were applied to 1 cm^2 and incubated at ambient conditions during 1 minute and the viral titer was evaluated; 30 min later a second drop was added on the same zone, and the viral titer was evaluated; 1 day later a third drop was added on the same zone and the viral titer was evaluated; 5 days later a fourth drop was added on the same zone and the viral titer was evaluated as described in the text. For experiments we used CH@AgCuNPs formulation in a dilution 1:3. The results show that none of these containers modified the biopolymer antiviral activity (**Table 3**).

2.6 Antibacterial activity

The antibacterial capacity of the CH@AgCuNPs -based formulation was estimated through the inhibition of the growth of gram-negative bacterium *E. coli*. As shown in **Figure 8**, bacterial exposure to increasing concentrations of the CH@AgCuNPs solutions resulted in a significant decrease in the OD_{600} measured for biopolymer concentrations equal to or greater than 0.1% v/v, which indicates inhibition of more than 95% of bacterial growth with respect to the untreated control (**Figure 8**). This result demonstrated that the CH@AgCuNPs solution has a deleterious effect on *E. coli*. Although intrinsic antimicrobial activity of CH has been extensively studied, this capacity is often potentiated by combination with metallic nanoparticles [47,48]. *E. coli* and *Staphylococcus aureus* are two representative pathogens that cause food decomposition as well as several infections [49]. Regarding biopolymers with a similar composition to our formulation, a recent investigation with CH-based films with embedded silver nanoparticles has reported inhibition of the culture growth of *S. aureus* [50]. Another study revealed that CH films with silver nanoparticles synthesized *in situ* exerted deleterious effects against *E. coli* and *S. aureus* [51]. Together, these studies demonstrate the multiple applications of CH biopolymers to control the growth of pathogenic bacteria. Since this work is focused on the development of coatings for facial masks in constant contact with the mouth, and which is a gateway for micro-organisms that can be harmful, the ability of biopolymers to inhibit their growth is of fundamental importance. More tests are needed to analyze the inhibitions on other types of bacteria or fungi.

Table 3. Evaluation of virus titers of CH@AgCuNPs stored in plastic container or glass container.

HSV-1 infectivity reduction (%)	plastic container	glass container
30 min	100,2±0,05	99,6±0,2
1 h	100,1±0,3	100,1±0,4
1 day	100 ± 0,2	100±0,3
5 days	100,1±0,3	99,8±1,2

2.7 Analysis of the biosafety of CH@AgCuNPs films

2.7.1 In vitro cytotoxicity studies

When developing implements for personal use that are in direct contact with the skin, a key aspect is to ensure biosecurity. The NRU is one of the most widely used tests to assess cytotoxicity in biomedicine that makes quantitative estimates of the number of living cells in culture. It is based on the ability of viable cells to incorporate and bind the neutral red supravital dye in lysosomes. Therefore, non-viable cells cannot incorporate the dye [52]. To ensure that the estimated parameters are within international standards, we adjusted our studies to the ISO 10993-5:2009 guideline "Biological evaluation of medical devices —Part 5:Tests for in vitro cytotoxicity". To analyze the biosafety of our developed CH formulation intended for masks coatings, Vero cells were exposed for 24 h to the extract of the films previously incubated in culture medium, to the culture medium alone, or 1% peroxide hydrogen as described in Experimental Section. NRU analysis showed that the treatment of Vero cells with 1% H_2O_2 (positive control for cell death) induced a highly significant decrease in cell viability (*** $P < 0.001$). Instead, the test revealed that there is no difference between the absorbance measured in the control condition with respect to the cells exposed to different concentrations (25 to100%) of the extracts of the CH@AgCuNPs film **(Figure 8A)**. These data suggest that there is no cytotoxic effect induced by CH@AgCuNPs in Vero cells culture.

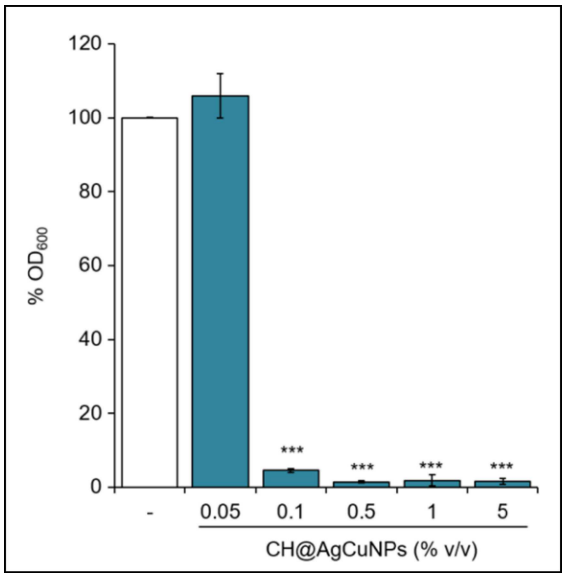

Figure 7. Antibacterial activity of CH@AgCuNPs on the *E. coli* bacteria. The bacteria were cultured at 37° C for 24 h with shaking in LB liquid medium supplemented with different concentrations of the CH@AgCuNPs. Bacterial growth was estimated by the optical density at 600 nm (OD_{600}). Means and SD are shown. ***P < 0.001 with respect to the control.

2.7.2 In vivo analysis of the Primary Dermal Irritation Index.

Since the CH@AgCuNPs films are intended for coating surfaces of masks in contact with the skin, we performed assays to evaluate possible irritating effects induced by the solid CH@AgCuNPs films as described in Materials and Methods. Erythema and edema readings at 1 h to 72 h of exposure revealed that the average score for all the individuals was zero for physiological solution or CH@AgCuNPs films. Figure 8b shows the integrity of the treated skin and the absence of signs

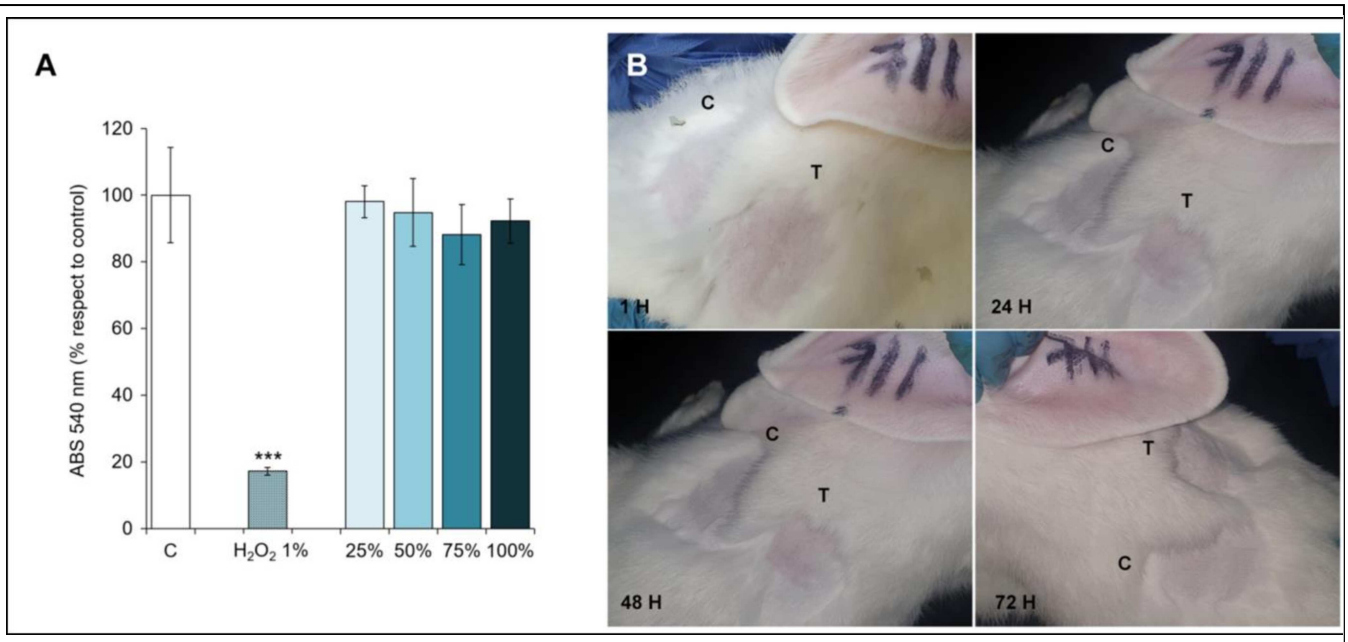

Figure 8. Biosafety analysis of the CH@AgCuNPs formulation. A) In vitro assessment of cytotoxicity. Vero cells were exposed for 24 h to increasing concentrations of the film-extracted medium or to 1% hydrogen peroxide. Cell viability was determined by NRU assay. Results are expressed as a percentage relative to the control of two independent experiments performed in quadruplicate. C: control condition. Means and SD are shown. ***P < 0.001 with respect to the control. B) Primary Dermal Irritation Index estimation. Albino rabbits were directly exposed to CH@AgCuNPs solid film in a shaved area for 1 to 72 h. In the same animal, other shaved area was used as control and treated with physiological solution. Representative images of the treated areas across the exposure times are shown.

of erythema or edema during the test. From these results, it can be concluded that the CH@AgCuNPs solid formulation is not irritating or corrosive to the skin and does not cause local or systemic adverse effects.

Conclusion

The studies performed show that the surfaces of the mask sprayed with CH@AgCuNPs formulations acquired antiviral and antibacterial effect as expected. Furthermore, the CH@AgCuNPs formulations resulted non-cytotoxic. Sprayed surfaces of the masks showed antiviral activity against HSV-1 and BCoV and reduced both virus titers about 100 %, while in untreated masks decline in viral titers was not observed. The action of CH@AgCuNPs formulations against these viruses was found to be fast and almost instantaneous. In view of these promising results, we consider that these CH@AgCuNPs formulations may be used not only for medical applications but also they might be applied in military, health care, work/uniforms, home fashions and domestic products, and sports apparel.

Experimental Section

1 Materials

All reagents used for the synthesis of the diverse - formulations based on chitosan were of analytical grade and used without further purifications. Chitosan-powered (Aparent viscosity 16MPA.S; deacetylation degree 95.37%) was provided by Farmacia Homeopática Pereda (Mar del Plata, Argentina). The glacial acetic acid (99.8% purity) was from Dorwill (Argentina) and copper sulfate pentahydrate ($CuSO_4$-$5H_2O$) (97% purity) and silver nitrate were purchased from Cicarelli (Argentina). In all the experiments distilled water was used.

The commercial face masks used in this work have three layers structure , in which a layer of textile is covered with non-woven bonded fabric on both sides. The material used to make these masks is polypropylene polystyrene, polycarbonate, polyethylene, or polyester.

2 Synthesis

A 3% CH solution was prepared by dissolving the required mass of biopolymer in in acetic acid (1%). In parallel, a 0.25% solution of $CuSO_4$ and $AgNO_3$ was prepared by dissolving the appropriated amount of these salts in distilled water.

The sprayable formulation was synthesized by mixing equal volumes of each solution employing a magnetic stirrer at room temperature during 1h.

After these procedures the concentrated formulation was obtained and an extra step of dilution was implemented to improve its spray ability, by adding distilled water in a relation 2:1 with respect to the concentrated formulation.

3 Characterization

3.1 Atomic absorption spectroscopy (AAS)

Cooper and silver content in the sprayable formulation was measured by atomic absorption spectroscopy using GBC Avanta 932 equipment.

3.2 X-ray diffraction (XRD)

X-ray Diffraction data were collected using a PANalytical Empyrean 3 diffractometer with Ni-filtered, CuKα radiation, and a PIXcel3D detector. It was operated at a current of 40 mA and a voltage of 45 kV. The data were collected using a continuous

scan mode with an angular speed of 2°/min for the angular range 5°≤ 2Θ ≤ 80°.

3.3 Fourier transform infrared spectroscopy (FTIR)

The incorporation of metallic moieties on the chitosan matrix was evaluated by Fourier Transform Spectroscopy, using a Thermo Scientific Nicolet iS50 in the frequency range of 400-4000 cm^{-1}. Previously to the measurements, samples were dried at room temperature and they were mixed with dry KBr powder and compacted.

3.4 TEM

Morphology was examined by transmission electron microscopy (TEM) using a JEOL 100 CX II, (JEOL, Tokyo, Japan 1983) microscopy. The samples were dispersed on 200 mesh Cu grids, and dried at room temperature and examined using different magnifications.

3.5. Z potential and hydrodynamic size

Data on hydrodynamic diameter and Z potential (ζ) were acquired in a Malvern Zetasizer (Nano-Zs90). Samples were diluted in distilled water and sonicated for one hour before performing the acquisition

4 Biological studies

4.1 Cell cultures

Vero cells (African green monkey kidney) (ATCC, CCL-81) and human colorectal adenocarcinoma cells (HRT-18: ATCC, CCL-244) were grown in Dulbecco's Modified Eagle's medium (DMEM, GIBCO) supplemented with 5% fetal bovine serum (Internegocios, Mercedes, Argentina) and were cultured at 37°C in 95% air with 5% CO_2 atmosphere. For maintenance of the Vero cell cultures, the serum concentration was reduced to 1.5% [53].

4.2 Viruses stock

HSV-1 strain Kos was propagated by infecting Vero cells. The cells were infected and incubated at 37 °C in an atmosphere containing 5% CO_2. Virus yield was determined by virus titration on fully confluent cells, by plaque-forming unit (PFU) technique [53].

Bovine betacoronavirus (BCoV, Mebus strain) stock preparation and titration assays were performed in HRT-18 cells, with the addition of 0.05% trypsin to the culture medium. BCoV titers were determined by microplate titration followed by immunofluorescence, using the method of Reed and Muench (1938) and were expressed as $TCID_{50}$ / ml. The titer of the viral stock was $10^{6.73}$ $TCID_{50}$ / ml and it was used at a concentration of 10^5 $TCID_{50}$ / ml.

4.3 BCoV adsorption and desorption assays

For the adsorption assay the CH@AgCuNPs (Gel chitosan-Cu 0,25%-Ag 0,25%) was evaluated undiluted and in 1:3 dilution. Dilutions were prepared in culture medium and then 40 µl of virus at 10^5 $TICD_{50}$/ml were added. Adsorption was carried out at room temperature with stirring for 30 minutes. After centrifugation at 16000 g for 5 minutes, the supernatant was collected for viral isolation. Titration in HRT18 cells was performed when cytopathic effect (CPE) was observed.

BCoV (10^5 $TCID_{50}$/ml) was incubated with severalsformulations for 30 minutes in a shaker and then was centrifugated at 16,000 g for 5 minutes. The obtained pellet was washed 3 times with PBS, and then 250 µl of 2M NaCl was added. After 30 min of desorption period in shaking, 100 µl of supernatant was collected, centrifuged at 16,000 g for 5 minutes, and the supernatant was titrated. A mixture of the virus with or without 2M NaCl was included as positive and negative control, respectively. To determine the percentage of virus desorbed from the biopolymer, the following formula was used: % desorbed virus = (viral titer in the supernatant of desorption assay/ viral titer in the virus control supernatant) X 100.

4.4 Sprayings assays on surfaces

CH formulations were used to CH@AgCuNPs spray-coat surfaces. Cleaned surfaces were used for coating. Firstly, the surfaces were sprayed with a handheld sprayer with CH formulations in a 1:2 or 1:3 dilution depositing approximately 100 µl/cm^2. When the CH formulations were dry, the surface was subjected to a UV cycle by 15 min and then viral infections were done.

4.5 Antiviral assay for HSV-1

CH@AgCuNPs -sprayed or unsprayed surfaces were virus or mock - infected at 1000 PFU in 20 µl for cm^2, then, inoculated surfaces were washed with 100 µl/1000 PFU of 2M NaCl at different times at 25 °C as described in our previous work [21]. Every sample was mixed for 15 minutes and then centrifuged for 1 min at 16000 rpm. Subsequently, HSV-1 was quantified in supernatants by plaque assay.

4.6 Plaque assay

Vero cells were cultured into 24-well microplates and grown overnight. Ten-fold dilutions of virus samples- CH@AgCuNPs formulations were added to monolayers of confluent Vero cells at 37°C for 1 h. Following incubation, the inoculum was removed, and monolayers overlaid with 1 ml of DMEM containing 1% methylcellulose. The cells were incubated at 37 °C for 48-72 hs and fixed using 4% formaldehyde. Finally, plaques were stained with 0.1% crystal violet in 20% ethanol and counted [53]. Control conditions were included where the untreated virus was incubated with Vero cells and finally, plaques were counted and percentage reduction in plaques formation in comparison to control wells was recorded as follows: % reduction = [(average viral titer in control condition − average viral titer in treated condition)/(average viral titer in the control condition)] × 100.

4.7 Determination of antibacterial properties

Gram-negative bacterium *Escherichia coli* (K12 strain RP437) were grown and maintained in a Luria-Bertani (LB) culture medium. The antibacterial action of the CH@AgCuNPs formulation spray was evaluated through the quantification of the optical density (OD_{600}) of *E. coli* cultures, after 24 h of exposure (37 ºC, 150 rpm). Five independent tests were carried out, with different concentrations of the CH@AgCuNPs solution. The control condition was the bacterial inoculum without CH solution. All treatments were carried out in duplicate. OD_{600} was measured at 24 hours, using a GeneQuant 1300 spectrophotometer (GE Healthcare).

4.8 Cytotoxicity analysis

Cytotoxicity of the solid films produced by CH@AgCuNPs formulations spraying was evaluated by the neutral red uptake assay (NRU) following the ISO 10993-5:2009 guideline. According to the procedures indicated in the guideline,

cytotoxicity was assessed indirectly by incubating the cells with the extracted medium of the films. To that end, the films were produced by direct spraying of 5 ml of CH@AgCuNPs solutions on watch glasses and after drying were sterilized by exposure to UV light for 30 minutes. The formed films were very thin, of insignificant thickness. Then 2 x 2 mm fragments were added to 5 ml of culture medium and incubated for 24 h at 37°C. The released medium was diluted and added to the cells in concentrations of 25 to 100%. In parallel, 2 x10^5 cells/well were seeded in 96 wells plates by quadruplicate. The cells were then treated for 24 hours with increasing concentrations of the extracts of the materials. As a control, the cells were incubated with the culture medium and as a positive control of cell death, 1% hydrogen peroxide carried in the culture medium was used. After treatment, the cells were washed with phosphate buffer pH 7.4 at 37° C and incubated with neutral red medium (NR medium): 1 ml stock solution 3% NR in 79 ml of DMEM 1.5% SFB. The selected serum concentration is optimal to avoid interference with the neutral red dye detections. After 3 hours of incubation with the NR medium, the cells were washed with phosphate buffer and the dye incorporated by the cells was extracted with a solution of 1% acetic acid, 50% distilled water, 49% ethanol 96°. Finally, absorbance at 540 nm was measured using a Biotek Synergy HT plate reader.

4.9 In vivo assessment of the Primary Dermal Irritation Index

In vivo studies were performed in accordance with the ARRIVE guidelines in an authorized laboratory (Laboratory enabled by the argentinian Ministry of Public Health by resolutions 2900-47228 - Disp. 0530; 001649 - Ley 11634 decreto 1443/2000; Disp. ANMAT Nro. 5892/15) . Three adult healthy albino rabbit (marks: 694 (3 kg weight) /697 (2.9 kg weight) /711 (2.4 kg weight) were used according to OECD 404 Methodology. Animals were individually housed at 21°C with 69% humidity and 12 hours artificial light-12 hours dark periods, fed with conventional laboratory diet (Ganave Grupo Pilar) and unrestricted supply of water. Primary Dermal Irritation Index was assessed through direct exposure of rabbit skin to solid CH@AgCuNPs films. The same rabbit that received a fraction of the solid biopolymer in a shaved area is used as a control by applying 0,5 ml of physiological solution in other shaved area in the opposite flank. After the application, both areas were covered with sterile gauze. Erythema and edema readings were made at the time of application, 24, 48 and 72 hours and the resulting average scoring according to the Draize test values (0 – 0.5: Not irritating; 0.5 – 1: Practically non-irritating; 1 – 2: Minimally irritating; 2 – 6: Moderately irritating; More than 6: Severely irritating) [54]> was used to classify the product.

5 Statistical analysis

GraphPad Prism software version 7 or 8 was used for all statistical analysis. The results represent the average of at least three experiments, with three or four dishes for each condition ± SEM, unless otherwise indicated. Statistical significance was determined by Student's two-tailed t-test or by ANOVA followed by Tukey's test with $p < 0.05$ considered significant.

Conflicts of interest

There are no conflicts to declare.

Acknowledgements

The authors thank to CONICET, FONARSEC (ANPCyT) Universidad Nacional del Sur and Universidad Nacional de Mar del Plata, Argentina.

Keywords: Chitosan biopolymer, coronavirus, HSV-1, face mask, antimicrobial

References

[1] H. Elachola, A. M. Assiri, Z. A. Memish, *Int. J. Infect. Dis.* **2014**, *20*, 77–78.
[2] O. Barasheed, M. Alfelali, S. Mushta, H. Bokhary, J. Alshehri, A. A. Attar, R. Booy, H. Rashid, *Int. J. Infect. Dis.* **2016**, *47*, 105–111.
[3] Q. Li, X. Guan, P. Wu, X. Wang, L. Zhou, Y. Tong, R. Ren, K. S. M. Leung, E. H. Y. Lau, J. Y. Wong, et al., *N. Engl. J. Med.* **2020**, *382*, 1199–1207.
[4] S.-Y. Ren, W.-B. Wang, Y.-G. Hao, H.-R. Zhang, Z.-C. Wang, Y.-L. Chen, R.-D. Gao, *World J. Clin. Cases* **2020**, *8*, 1391–1399.
[5] N. M. Wilson, A. Norton, F. P. Young, D. W. Collins, *Anaesthesia* **2020**, *75*, 1086–1095.
[6] N. van Doremalen, T. Bushmaker, D. H. Morris, M. G. Holbrook, A. Gamble, B. N. Williamson, A. Tamin, J. L. Harcourt, N. J. Thornburg, S. I. Gerber, et al., *N. Engl. J. Med.* **2020**, *382*, 1564–1567.
[7] R. Sommerstein, C. A. Fux, D. Vuichard-Gysin, M. Abbas, J. Marschall, C. Balmelli, N. Troillet, S. Harbarth, M. Schlegel, A. Widmer, et al., *Antimicrob. Resist. Infect. Control* **2020**, *9*, 100.
[8] P. Yang, H. Seale, C. Raina MacIntyre, H. Zhang, Z. Zhang, Y. Zhang, X. Wang, X. Li, X. Pang, Q. Wang, *Brazilian J. Infect. Dis.* **2011**, *15*, 102–108.
[9] N. H. L. Leung, D. K. W. Chu, E. Y. C. Shiu, K.-H. Chan, J. J. McDevitt, B. J. P. Hau, H.-L. Yen, Y. Li, D. K. M. Ip, J. S. M. Peiris, et al., *Nat. Med.* **2020**, *26*, 676–680.
[10] H. Wu, J. Huang, C. J. P. Zhang, Z. He, W.-K. Ming, *EClinicalMedicine* **2020**, *21*, 100329.
[11] M. H. Chua, W. Cheng, S. S. Goh, J. Kong, B. Li, J. Y. C. Lim, L. Mao, S. Wang, K. Xue, L. Yang, et al., *Research* **2020**, *2020*, 1–40.
[12] WHO, "World Health Organization (WHO) Shortage of personal protective equipment endangering health workers worldwide," can be found under https://www.who.int/news-room/detail/03-03-2020-shortage-of-personal-protective-equipment-endangering-health-workers-worldwide, **2020**.
[13] G. E. De-la-Torre, D. C. Dioses-Salinas, C. I. Pizarro-Ortega, M. D. Fernández Severini, A. D. Forero López, R. Mansilla, F. Ayala, L. M. J. Castillo, E. Castillo-Paico, D. A. Torres, et al., *J. Hazard. Mater.* **2022**, *426*, 128070.
[14] V. N. Davydova, V. P. Nagorskaya, V. I. Gorbach, A. A. Kalitnik, A. V. Reunov, T. F. Solov'eva, I. M. Ermak, *Appl. Biochem. Microbiol.* **2011**, *47*, 103–108.
[15] N. Jaber, M. Al-Remawi, F. Al-Akayleh, N. Al-Muhtaseb, I. S. I. Al-Adham, P. J. Collier, *J. Appl. Microbiol.* **2022**, *132*, 41–58.
[16] L. O. Cinteza, C. Scomoroscenco, S. N. Voicu, C. L. Nistor, S. G. Nitu, B. Trica, M. L. Jecu, C. Petcu, *Nanomaterials* **2018**, *8*, DOI 10.3390/nano8100826.
[17] P. K. Dara, R. Mahadevan, P. A. Digita, S. Visnuvinayagam, L. R. G. Kumar, S. Mathew, C. N. Ravishankar, R. Anandan, *SN Appl. Sci.* **2020**, *2*, 665.
[18] R. Kalaivani, M. Maruthupandy, T. Muneeswaran, A. Hameedha Beevi, M. Anand, C. M. Ramakritinan, A. K. Kumaraguru, *Front. Lab. Med.* **2018**, *2*, 30–35.
[19] Y. Mori, T. Ono, Y. Miyahira, V. Q. Nguyen, T. Matsui, M. Ishihara, *Nanoscale Res. Lett.* **2013**, *8*, 93.
[20] F. Buazar, S. Sweidi, M. Badri, F. Kroushawi, *Green Process. Synth.* **2019**, *8*, 691–702.
[21] M. F. Favatela, J. Otarola, V. B. Ayala-Peña, G. Dolcini, S. Perez, A. Torres Nicolini, V. A. Alvarez, V. L. Lassalle, *J.*

Inorg. Organomet. Polym. Mater. **2022**, *32*, 1473–1486.
[22] N. Bouazizi, J. Vieillard, P. Thebault, F. Desriac, T. Clamens, R. Bargougui, N. Couvrat, O. Thoumire, N. Brun, G. Ladam, et al., *Dalt. Trans.* **2018**, *47*, 9143–9155.
[23] R. E. Morsi, A. M. Alsabagh, S. A. Nasr, M. M. Zaki, *Int. J. Biol. Macromol.* **2017**, *97*, 264–269.
[24] D. S. More, M. J. Moloto, N. Moloto, K. P. Matabola, *Int. J. Polym. Sci.* **2021**, *2021*, 1–12.
[25] C. Jin, B. Yu, J. Zhang, H. Wu, X. Zhou, H. Yao, F. Liu, X. Lu, L. Cheng, M. Jiang, et al., *BMC Infect. Dis.* **2021**, *21*, 672.
[26] S. Khaiboullina, T. Uppal, N. Dhabarde, V. R. Subramanian, S. C. Verma, *Viruses* **2020**, *13*, 19.
[27] L.-S. Wang, S. Xu, S. Gopal, E. Kim, D. Kim, M. Brier, K. Solanki, J. S. Dordick, *Sci. Rep.* **2021**, *11*, 12410.
[28] K. Ravishankar, R. Dhamodharan, *React. Funct. Polym.* **2020**, *149*, 104517.
[29] C. Saldías, D. D. Díaz, S. Bonardd, C. Soto-Marfull, A. Cordoba, S. Saldías, C. Quezada, D. Radic, Á. Leiva, *Carbohydr. Polym.* **2018**, *180*, 200–208.
[30] M. Kozicki, M. Kołodziejczyk, M. Szynkowska, A. Pawlaczyk, E. Leśniewska, A. Matusiak, A. Adamus, A. Karolczak, *Carbohydr. Polym.* **2016**, *140*, 74–87.
[31] T. Abiraman, E. Ramanathan, G. Kavitha, R. Rengasamy, S. Balasubramanian, *Ultrason. Sonochem.* **2017**, *34*, 781–791.
[32] F. Khoerunnisa, Y. D. Yolanda, M. Nurhayati, F. Zahra, M. Nasir, P. Opaprakasit, M.-Y. Choo, E.-P. Ng, *Inventions* **2021**, *6*, 98.
[33] K. S. Zerda, C. P. Gerba, K. C. Hou, S. M. Goyal, *Appl. Environ. Microbiol.* **1985**, *49*, 91–95.
[34] J. Ciejka, K. Wolski, M. Nowakowska, K. Pyrc, K. Szczubiałka, *Mater. Sci. Eng. C* **2017**, *76*, 735–742.
[35] A. Milewska, J. Ciejka, K. Kaminski, A. Karewicz, D. Bielska, S. Zeglen, W. Karolak, M. Nowakowska, J. Potempa, B. J. Bosch, et al., *Antiviral Res.* **2013**, *97*, 112–121.
[36] A. Milewska, M. Zarebski, P. Nowak, K. Stozek, J. Potempa, K. Pyrc, *J. Virol.* **2014**, *88*, 13221–13230.
[37] X. Mi, K. S. Vijayaragavan, C. L. Heldt, *Carbohydr. Res.* **2014**, *387*, 24–29.
[38] A. Karger, J. Schmidt, T. C. Mettenleiter, *J. Virol.* **1998**, *72*, 7341–7348.
[39] M. Hosseini, A. W. H. Chin, S. Behzadinasab, L. L. M. Poon, W. A. Ducker, *ACS Appl. Mater. Interfaces* **2021**, *13*, 5919–5928.
[40] G. A. Sotiriou, S. E. Pratsinis, *Environ. Sci. Technol.* **2010**, *44*, 5649–5654.
[41] G. A. Sotiriou, A. Meyer, J. T. N. Knijnenburg, S. Panke, S. E. Pratsinis, *Langmuir* **2012**, *28*, 15929–15936.
[42] C. Gunawan, M. B. Faiz, R. Mann, S. R. S. Ting, G. A. Sotiriou, C. P. Marquis, R. Amal, *ACS Appl. Mater. Interfaces* **2020**, *12*, 5557–5568.
[43] G. Borkow, J. Gabbay, *Curr. Med. Chem.* **2005**, *12*, 2163–2175.
[44] J. Hodek, V. Zajícová, I. Lovětinská-Šlamborová, I. Stibor, J. Müllerová, J. Weber, *BMC Microbiol.* **2016**, *16*, 56.
[45] M. Rai, A. Yadav, A. Gade, *Biotechnol. Adv.* **2009**, *27*, 76–83.
[46] H. H. Lara, E. N. Garza-Treviño, L. Ixtepan-Turrent, D. K. Singh, *J. Nanobiotechnology* **2011**, *9*, 30.
[47] J. Li, S. Zhuang, *Eur. Polym. J.* **2020**, *138*, 109984.
[48] M. Malini, M. Thirumavalavan, W.-Y. Yang, J.-F. Lee, G. Annadurai, *Int. J. Biol. Macromol.* **2015**, *80*, 121–129.
[49] B. Hilmi, Y. Bustami, T. Trongsatitkul, Z. A. Abdul Hamid, *J. Phys. Sci.* **2019**, *30*, 55–63.
[50] N. Mohamed, N. G. Madian, *Mater. Today Commun.* **2020**, *25*, 101372.
[51] B. Gu, Q. Jiang, B. Luo, C. Liu, J. Ren, X. Wang, X. Wang, *Carbohydr. Polym.* **2021**, *260*, 117835.
[52] G. Repetto, A. del Peso, J. L. Zurita, *Nat. Protoc.* **2008**, *3*, 1125–1131.
[53] V. Ayala-Peña, G. Santillán, L. Scolaro, *Biochem. Biophys. Res. Commun.* **2014**, *451*, 609–614.
[54] R. G. Tardiff, R. P. Hubner, C. Gevecker Graves, *J. Appl. Toxicol.* **2003**, *23*, 279–281.

Entry for the Table of Contents

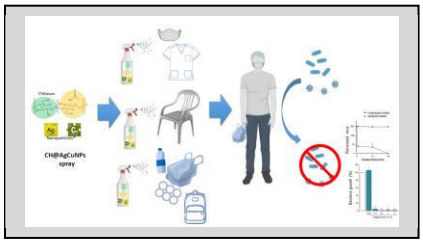

In this work, we develop novel, simple and scalable methods to obtain low-density CH-based formulations containing Ag and CuO nanoparticles. This spray resulted non-cytotoxic and easy application to avoid the spread of certain viruses and bacteria.